MABS
2016, VOL. 8, NO. 3, 562–573
http://dx.doi.org/10.1080/19420862.2016.1147640

Taylor & Francis
Taylor & Francis Group

REPORT

OPEN ACCESS

Anti-tumoral, anti-angiogenic and anti-metastatic efficacy of a tetravalent bispecific antibody (TAvi6) targeting VEGF-A and angiopoietin-2

Werner Scheuer[a], Markus Thomas[a], Petra Hanke[a], Johannes Sam[b], Franz Osl[a], Diana Weininger[a], Monika Baehner[a], Stefan Seeber[a], Hubert Kettenberger[a], Jürgen Schanzer[a], Ulrich Brinkmann[a], K. Michael Weidner[a], Jörg Regula[a], and Christian Klein[b]

[a]Roche Innovation Center Penzberg, Roche Pharma Research and Early Development, Nonnenwald 2, Penzberg, Germany; [b]Roche Innovation Center Zurich, Roche Pharma Research and Early Development, Wagistrasse 18, Schlieren, Switzerland

ABSTRACT

Vascular endothelial growth factor (VEGF)-A blockade has been validated clinically as a treatment for human cancers. Angiopoietin-2 (Ang-2) is a key regulator of blood vessel remodeling and maturation. In tumors, Ang-2 is up-regulated and an unfavorable prognostic factor. Recent data demonstrated that Ang-2 inhibition mediates anti-tumoral effects. We generated a tetravalent bispecific antibody (Ang-2-VEGF-TAvi6) targeting VEGF-A with 2 arms based on bevacizumab (Avastin®), and targeting Ang-2 with 2 arms based on a novel anti-Ang-2 antibody (LC06). The two Ang-2-targeting single-chain variable fragments are disulfide-stabilized and fused to the C-terminus of the heavy chain of bevacizumab. Treatment with Ang-2-VEGF-A-TAvi6 led to a complete abrogation of angiogenesis in the cornea micropocket assay. Metastatic spread and tumor growth of subcutaneous, orthotopic and anti-VEGF-A resistant tumors were also efficiently inhibited. These data further establish Ang-2-VEGF bispecific antibodies as a promising anti-angiogenic, anti-metastatic and anti-tumor agent for the treatment of cancer.

ARTICLE HISTORY
Received 18 September 2015
Revised 20 January 2016
Accepted 25 January 2016

KEYWORDS
Angiopoietin-2; bispecific; BsAb; scFv; VEGF-A

Introduction

Anti-angiogenic therapies have emerged over the last few years as an important part of anti-cancer therapies. The main targets of clinically approved anti-angiogenic drugs are vascular endothelial growth factor (VEGF)-A and VEGF receptors (VEGFR). However, clinical experience shows that the efficacy of such therapies is limited due to overlapping and compensatory alternative angiogenic pathways which provide escape mechanisms.[1,2] Therefore, alternatives are needed to improve survival of cancer patients. A detailed understanding of the molecular and cellular mode of action of anti-VEGF/R therapies could provide a rationale for combination therapies with other targeted agents and chemotherapies. Recently, there has also been great interest in combining immunotherapies with anti-angiogenic therapy.[3] Knowledge from such studies would facilitate the optimization of treatment schedules[4] and support research activities focused on identifying biomarkers to predict which patients will benefit from anti-VEGF therapy.[5]

One mechanism to circumvent resistance concentrates on the up-regulation of other pro-angiogenic factors. In preclinical models it has been demonstrated that tumor cells can bypass endogenous angiogenesis inhibitors by up-regulating Ang-2.[6] More importantly, preclinical and clinical anti-VEGF-A treatment induces upregulation of Ang-2.[7-10] Thus, inhibition of Ang-2 suppresses growth of tumors in preclinical models and such treatments correlate with a reduction of tumor-associated blood vessels.[11-17] Consequently, Ang-2 is now considered a promising target in cancer patients.[18] Recently, it was demonstrated that the combined treatment of Ang-2 inhibition with an anti-VEGF-A antibody led to an almost complete inhibition of tumor growth.[19] With the advent of bispecific antibody engineering, it is now possible to combine 2 targeting molecules in one. Recently this technology was applied in 2 different approaches to neutralize VEGF-A and Ang-2 simultaneously.[8,20] Both bispecific antibodies, CVX-241 and Ang-2-VEGF-A CrossMab (RG7221, vanucizumab), suppressed tumor growth and reduced micro vessel density. In combination with chemotherapy, a synergistic effect on tumor volume was demonstrated. While CVX-241 is no longer in clinical development, vanucizumab is currently in Phase 2 clinical trials in direct comparison to bevacizumab in combination with chemotherapy (NCT02141295). Apart from providing pharmacoeconomic advantages by applying a bispecific antibody instead of a combination, Ang-2-VEGF bispecific antibodies also provide the advantage of blocking both pathways simultaneously from the beginning of therapy, and may thus avoid tumor escape mechanisms.

Here, we describe an alternative tetravalent bispecific antibody (TAvi6) targeting VEGF-A based on bevacizumab (Avastin®) that also targets Ang-2 by 2 disulfide-

CONTACT Dr. Christian Klein christian.klein.ck1@roche.com

stabilized single-chain variable fragments (scFvs; LC06) fused to the C-terminus of the heavy chain of bevacizumab. TAvi6 was evaluated not only regarding its efficacy on tumor growth in different human xenografts, but also as second-line therapy in a model in which tumors have progressed under monotherapy with bevacizumab. More importantly, the effect of TAvi6 on metastasis was assessed. This issue has attracted considerable interest because recent preclinical studies suggest that adjuvant VEGF therapies may increase the risk of metastasis.[21-23] Finally, we monitored the effect of TAvi6 on vascular formation by a non-invasive optical imaging method after an intravenous (i.v.) injection of a fluorescence-labeled antibody against CD31.

Results

TAvi6 production (purification), stability, formulation and CHO clone generation

Ang-2-VEGF-A-TAvi6 is an IgG1-like monoclonal antibody based on bevacizumab with an angiopoietin-binding scFv fused to the C-termini of the heavy chains (Fig. 1A). The scFv is derived from the parental antibody LC06, which selectively binds Ang2. It possesses a more than 100-fold lower affinity for Ang1 than for Ang2. Based on experiences

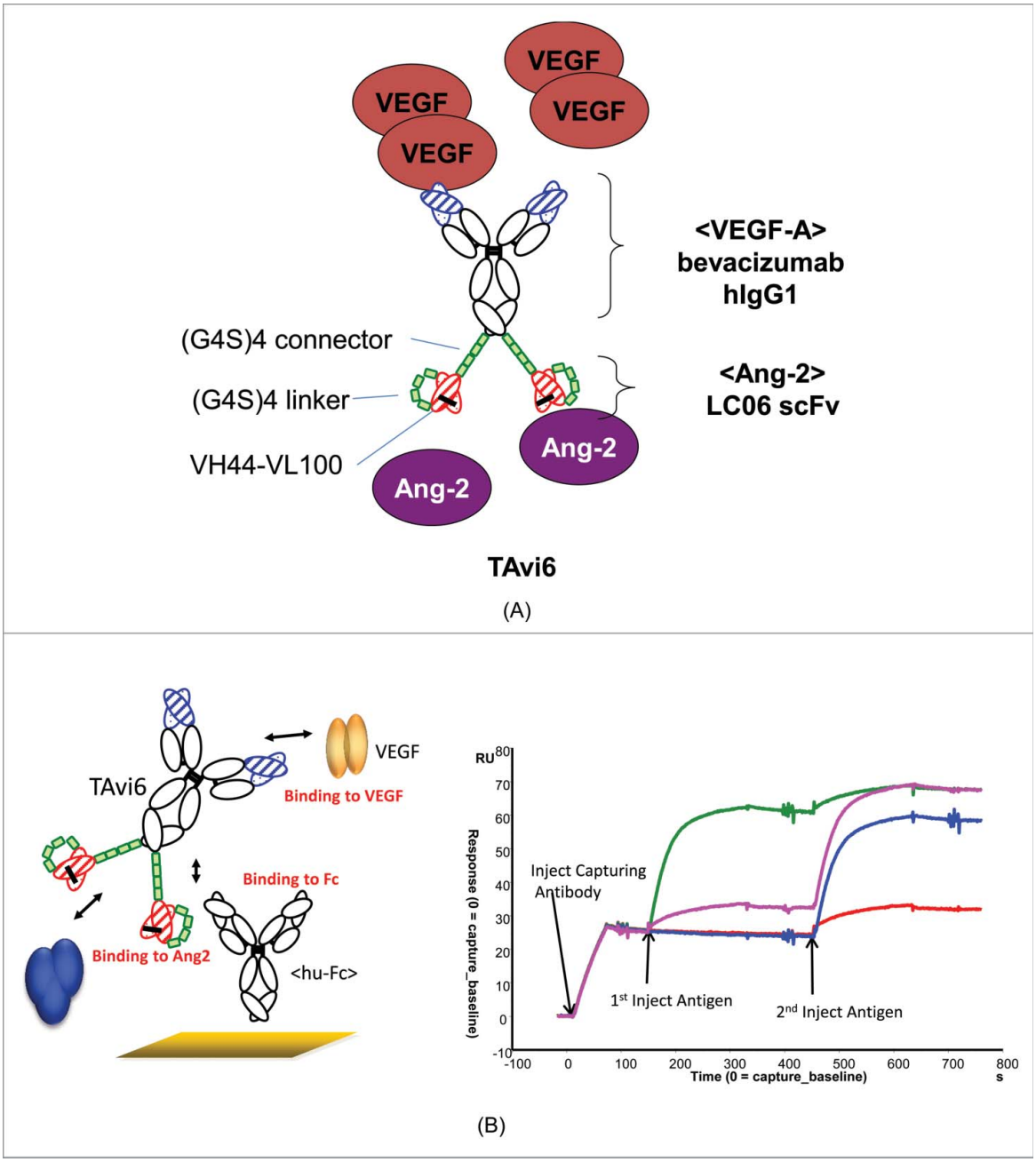

Figure 1. (A) Scheme of Ang-2-VEGF-A-TAvi6 tetravalent antibody. (B) Schematic representation of the SPR assay demonstrating the functional properties of TAvi6 and its ability for simultaneous and independent binding. Green: Ang-2 followed by VEGF, Magenta: VEGF followed by Ang-2, Blue: Buffer followed by Ang-2, Red: Buffer followed by VEGF.

with other bispecific IgG-scFv fusions, the C-terminal scFvs were connected via a $(G_4S)_4$ linker and were disulfide stabilized (Vh44-Vl100) to avoid dimerization and aggregation via daisy chains.[24-29] The bispecific antibody is stable and can be produced by transient expression with yields of about 60 mg/L. TAvi6 can be purified via industry-standard methods routinely used for conventional IgG antibodies and previously described for bispecific antibodies,[27-29] starting with a Protein A affinity chromatography step. Depending on the scale, either a size-exclusion or cation- and anion-exchange chromatography steps can be utilized to purify the antibody. The aggregation onset temperature was determined with 63°C. For the studies described here, transiently expressed TAvi6 was used, while for large scale production a stable Chinese hamster ovary (CHO) cell line with a volumetric productivity of ca 1.2 g/L was generated (data not shown).

The functionality of TAvi6 was assessed via surface plasmon resonance (SPR) experiments, as well as cell-based and cell-free functional assays. The dimeric and oligomeric nature of both ligands together with the bivalency of TAvi6 for the respective targets is a challenge and needs to be considered when interpreting the results. We used SPR experiments to determine the species cross-reactivity and the binding properties of both soluble ligands Ang2 and VEGF. One important feature of TAvi6 is its ability to bind both ligands simultaneously and independent of the order, as demonstrated by SPR (Fig. 1B). The affinities for Ang2 are in the low nM range and the Ang2 binding domain is cross-reactive toward cynomolgus monkey and the murine target. The VEGF binding domain does not cross-react with murine VEGF, which needs to be considered when interpreting in vivo experiments. The different affinities are summarized in Table 1. Additional insights into the functional properties of the TAvi6 molecules come from the Ang2-Tie2 interaction ELISA and FACS assay, as well as the Tie2 phosphorylation assay (Table 2). All assays indicated IC50 values in the low nM range and showed that the TAvi6 antibody is capable of blocking the interaction between Ang2 and Tie2. The VEGF-VEGFR interaction was analyzed with the VEGF-VEGFR interaction ELISA, as well as with the HUVEC proliferation assay. Both assays showed that the VEGF-VEGFR interaction was blocked by bevacizumab. We concluded that the functional properties of the parental antibodies are maintained in the TAvi6 molecule.

Single dose pharmacokinetic (PK) studies in non-tumor-bearing mice showed that TAvi6 possessed typical IgG1 like PK properties with a terminal half-life of 163h, clearance of 0.0058mL/min/kg and a distribution volume of 0.0775 L/kg. Subsequently, TAvi6 was tested in different in vivo xenograft models in comparison to the respective parental antibodies bevacizumab and LC06 and the combination thereof. Its biological properties in in vivo angiogenesis and tumor models are described below.

Table 1. Affinities and cross-reactivity of TAvi6.

	human Target K_D [nM]	Cynomolgus Target K_D [nM]	Murine Target K_D [nM]
Ang2	0.7*	1.2*	0.6*
VEGF	<0.1*	<0.1*	no binding

Table 2. Functional properties of TAvi6 in vitro.

Ang2 blocking properties of TAvi6	
Ang2 specific assays	IC50 [nM]
hANGPT2-Tie2 interaction ELISA	IC50 = 330 ng/ml (1–3 nM)
hANGPT2-Tie2 ligand binding FACS	IC50 = 330 ng/ml (1–3 nM)
ANGPT2 induced Tie2 phosphorylation	IC50 = 300-400 ng/ml (1–3 nM)
VEGF blocking properties of TAvi6	
hVEGF-VEGFR interaction ELISA	IC50 = 2830 ng/ml (13.9 nM)
VEGF induced HUVEC proliferation IC50	= 640 ng/ml (3 nM)

(*low sensitivity assay).

TAvi6 inhibits human VEGF-A induced angiogenesis in mouse cornea micropocket assay

Angiogenesis was induced by implanting VEGF-A soaked nylaflo discs into the cornea of BALB/c mice. In contrast to the phosphate-buffered saline (PBS)-soaked control discs, VEGF-A induced vessel outgrowth from the limbus to the disc. Systemic administration of bevacizumab and TAvi6 significantly inhibited VEGF-A induced neoangiogenesis during the observation period from day 3 to day 7, whereas treatment with the anti-Ang-2 antibody LC06 was effective on days 5 and 7. Taken together, TAvi6 suppressed angiogenesis more efficiently than the monospecific treatments (Fig. 2, Table 3).

TAvi6 mediates strong anti-tumoral efficacy in different human xenograft models

The compounds were tested in 3 different xenograft models. Table 4 summarizes the data. In the Colo205 xenograft model, tumor growth inhibition (TGI) at the endpoint was 66% for bevacizumab (10 mg/kg, qwx7, $p < 0.001$, TCR = 0.46, CI = 0.19−0.80); 47% for LC06 (10 mg/kg, qwx7, $p = 0.032$, TCR = 0.61, CI = 0.33−0.99); 78% for the combination of bevacizumab and LC06 (10 mg/kg, qwx7 for each antibody, $p < 0.001$, TCR = 0.32, CI = 0.04−0.65) and 87% using a matched dose of TAvi6 (13.3 mg/kg, qwx7, $p = 0.001$, TCR = 0.28 CI = 0.02−0.59) (Fig. 3A). In this study, TAvi6 was compared to muTAvi, an analogous bispecific antibody containing the murine/human VEGF cross-reactive VEGF antibody B20-4.1 (13.3 mg/kg, qwx7)[30] and to Ang-2-VEGF-CM, a bispecific Ang-2-VEGF CrossMAb based on LC06 and bevacizumab, monovalent for its 2 targets at a matched dose (20 mg/kg, qwx7).[31] In this model, both antibodies showed anti-tumor efficacy comparable to that of TAvi6 and the combination of bevacizumab and LC06 with a TGI of 86% for muTAvi6 (TCR = 0.50, CI = −0.23−0.85) and a TGI of 93% for Ang-2-VEGF-CM (TCR = 0.20, CI = −0.07−0.49) (data not shown).

In the orthotopic KPL-4 xenograft model using the equivalent dose and schedule, TGI at the endpoint was 79% for bevacizumab ($p = 0.004$, TCR = 0.22, CI = −0.10–0.61); 39% for LC06 (not significant, TCR = 0.83 CI = 0.46–1.43); 90% for the combination ($p = 0.003$, TCR = 0.12, CI = −0.23–0.51) and 91% for TAvi6 ($p = 0.002$, TCR = 0.11, CI = −0.23–0.47) (Fig. 3B).

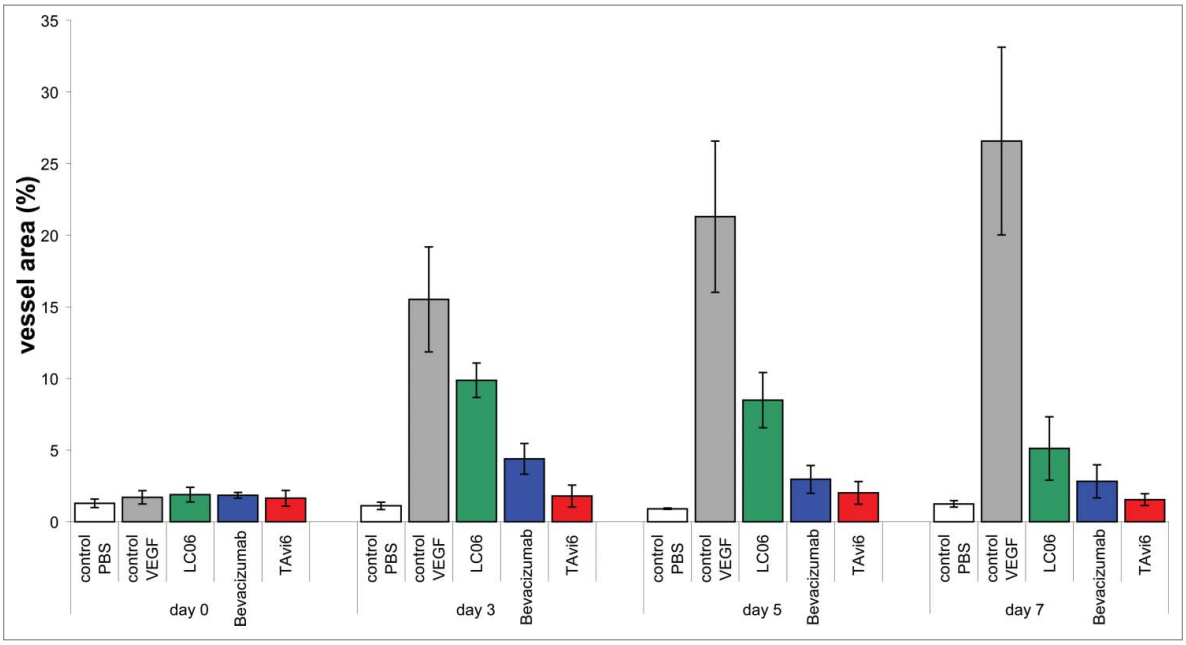

Figure 2. Corneal micropocket model. PBS and VEGF-A containing discs were implanted in the corneal pocket of mice and mice were treated with vehicle, LC06, bevacizumab and TAvi6 with 10 mg/kg i.v. on the day of disc implantation. Vessel area was quantified by calculating the area of new vessels as a fraction of the total area of the cornea.

In the Calu-3 xenograft model using the equivalent dose and schedule, treatment with bevacizumab resulted in a TGI of 60% ($p = 0.006$, nTCR = 0.38, CI = 0.13–0.69), for LC06 the TGI was 55% ($p = 0.007$, TCR = 0.43, CI = 0.18−0.76), the combination mediated a TGI of 65% ($p = 0.004$, TCR = 0.33, CI = 0.08–0.64) and TAvi6 mediated a TGI of 70% ($p < 0.001$, TCR = 0.25, CI = 0.00–0.54) (Fig. 3C).

In all studies the combination of bevacizumab with LC06 as well as TAvi6 were significantly different from the vehicle-treated control group, but there were no significant differences between the combination of both antibodies and TAvi6 treatment. While TAvi6 mediated the best anti-tumoral efficacy in all these studies, the confidence intervals overlapped with the respective single agent therapies.

Table 3. Corneal angiogenesis model.

		%Inhibition	p
day3	LC06	36.4	0.177
	Bevacizumab	71.7	0.017
	TAvi6	88.4	0.002
day5	LC06	60.1	0.048
	Bevacizumab	86.1	0.008
	TAvi6	90.5	0.003
day7	LC06	80.7	0.013
	Bevacizumab	89.4	0.006
	TAvi6	94.2	0.002

Micropockets were prepared at ~1 mm from the limbus to the top of the cornea in the anesthetized mice. The disc were implanted and incubated with the corresponding growth factor or with vehicle for at least 30 min. After 5 days, eyes were photographed and vascular response was measured. The assay was quantified by calculating the area of new vessels as a fraction of the total area of the cornea. Results were expressed as mean±SEM. Differences between experimental groups were analyzed by unpaired Student's t-test. P values < 0.05 were considered statistically significant.

TAvi6 inhibits growth of tumors refractory to treatment with bevacizumab

Established Colo205 xenografts were treated with 10 mg/kg bevacizumab intraperitoneally (i.p.) administered once weekly for 5 weeks. Thereafter, mice were randomized into 4 study groups based on tumor volume. Study groups were either treated once weekly (10 mice/group) with bevacizumab or LC06 or bevacizumab + LC06 or with TAvi6. Compared to bevacizumab maintenance treatment, LC06 suppressed tumor volume by 44% ($p = 0.006$), the combination of bevacizumab and LC06 45% ($p = 0.005$), and for TAvi6 the TGI was 60% ($p=0.002$) (Fig. 4A). The results demonstrate the predominant role of angiopoietin-2 under anti-VEGF-A treatment. We previously demonstrated in Colo205 tumors that anti-VEGF-A treatment leads to an upregulation of tumor-derived Ang-2 as a potential mechanism of resistance.[8] Histology of explanted tumors revealed massive destruction of tumor cells after TAvi6 treatment (Fig. 4B). Therefore, TAvi6 was able to suppress growth of tumors that had become refractory to first-line treatment with bevacizumab.

TAvi6 suppresses tumor cell dissemination to the lung in the subcutaneous Colo205 CRC xenograft after first-line bevacizumab

It was shown previously that targeting the Ang-2/Tie2 axis inhibits metastasis formation.[6,8,15] Therefore, we analyzed tumor cell dissemination to the lung in the first-line bevacizumab-treated mice. At termination of the Colo205 study (day 91), lungs were collected from animals of all groups for quantification of human DNA. Human Alu-specific

Table 4. Anti-tumor efficacy in xenograft models. Tumor growth inhibition (TGI) and non-parametric Tumor-Control Ratio (TCR) with 95% Confidence Interval (CI) are shown.

	Colo205 TGI TCR, CI	KPL-4 TGI (TCR, CI)	Calu-3 TGI (TCR, CI)
Bevacizumab	66% TCR=0.46, CI=0.19–0.80	79% TCR=0.22, CI=−0.10–0.61	60% nTCR=0.38, CI=0.13–0.69
LC06	47% TCR=0.61, CI=0.33–0.99	39% TCR=0.83 CI=0.46–1.43	55% TCR=0.43, CI=0.18–0.76
Bevacizumab + LC06	78% TCR=0.32, CI=0.04–0.65	90% TCR=0.12, CI=−0.23–0.51	65% TCR=0.33, CI=0.08–0.64
TAvi6	87% TCR=0.28 CI=0.02–0.59	91% TCR=0.11, CI=−0.23–0.47	70% TCR=0.25, CI=0.00–0.54
muTAvi6	86% TCR=0.50, CI=−0.23–0.85	not determined	not determined
Ang-2-VEGF-CM	93% TCR=0.20, CI=−0.07–0.49	not determined	not determined

primers were chosen for selective amplification of Alu sequences by quantitative PCR. Compared to the bevacizumab-treated group as well as LC06, bevacizumab + LC06, TAvi6 significantly suppressed the dissemination of tumor cells to the lung in a similar efficacy range (TAvi6 suppression was 66%) (Fig. 4C).

TAvi6 efficiently inhibits angiogenesis in the Calu-3 NSCLC xenograft model

Mice bearing subcutaneous (s.c.) Calu-3 tumors were subsequently injected with 2 mg/kg fluorescence-labeled anti-CD31 i.v. on days 34 and 78 to image vessels. Fluorescence signal intensities were measured by planar reflectance imaging 24 hrs thereafter (MAESTRO; CRi) (Fig. 5A). In the omalizumab treatment group, the signal intensity became more prominent from day 35 to day 79, indicating the presence of more CD31-positive vessels in the tumor tissue, and thus permitting us to conclude that vessel formation has occurred. In contrast, treatment with the combination of bevacizumab plus LC06 or with TAvi6 significantly reduced fluorescence intensities in the region of interest. The relative changes of CD31 staining were assessed. Treatment groups exhibited no significant changes of labeled anti-CD31 signals in the first 2 weeks of treatment (yellow bars: day 35 to day 47). In contrast, fluorescence signal intensities declined in the combination and the TAvi6 treated groups of mice indicating that vessel formation was affected by these treatments (red bars: days 47 to 79) (Fig. 5B). After the last in vivo imaging (day 79), tumors were explanted for histological examination. Slides were evaluated by classical histology (HE) and multispectral fluorescence microscopy (NUANCE; CRi). Compared to the omalizumab group, a high number of dead tumor cells in the TAvi6 treated mice was detected (95% vs 50%). Based on fluorescence microscopy, vessel sizes and vessel densities were quantified manually in 3 tumors from each group and 4 slides from each tumor were analyzed. Compared to omalizumab, all treatments suppressed vessel densities significantly (bevacizumab $p = 0.029$; bevacizumab+LC06 $p = 0.001$) and TAvi6 exerted the most prominent effect (75% inhibition, $p = 0.001$) (Fig. 5C), but there was no significant difference between TAvi6 and bevacizumab+LC06.

Discussion

In this study, we describe the generation and therapeutic efficacy of a novel tetravalent IgG-like bispecific antibody targeting VEGF-A and Ang-2 simultaneously. This TAvi6 bispecific antibody of the IgG1 isotype showed IgG-like pharmacokinetic properties and stability and can be produced using standard processes in a CHO cell line with yields > 1 g/L. TAvi6 significantly blocked human VEGF-A stimulated angiogenesis in mouse cornea micropocket assay more efficiently than single treatment with anti-Ang2 or bevacizumab. Significant anti-tumoral efficacy by weekly injection of TAvi6 was demonstrated in 3 different xenograft models (Colo205, KPL-4 and Calu-3). No clinical signs of toxicity such as weight loss or behavioral changes were observed during these efficacy studies. When interpreting these data it has to be kept in mind that, whereas in xenograft models the anti-Ang-2 LC06 variable region blocks primarily host-derived endothelial murine Ang-2, the anti-VEGF bevacizumab variable region only blocks tumor cell-derived human VEGF. In order to model the mechanism of action closest to the human situation, use of a murine/human VEGF cross-reactive antibody in TAvi6 is required.

We compared TAvi6 with muTAvi6, an analogous bispecific antibody that also recognizes muVEGF, but did not observe enhanced anti-tumoral efficacy in the Colo205 model, indicating that angiogenesis in this model is largely driven by human VEGF secreted by the tumor cells.[8] Nevertheless, it can be assumed that the anti-tumoral and anti-angiogenic action on TAvi6 in xenograft models is not fully reflected due to its lack of recognition of muVEGF. We also compared TAvi6 to Ang-2-VEGF-CM, a bispecific Ang-2-VEGF CrossMAb based on LC06 and bevacizumab, monovalent for its 2 targets at a matched dose, and did not observe major differences in their anti-tumoral efficacy, indicating that bivalency for VEGF and/or Ang-2 did not result in superior activity in the Colo205 model.

Tumors can escape anti-angiogenic treatment due to the up-regulation of additional angiogenic signaling pathways, for example, by upregulation of Ang-2.[6] Evaluation of second-line therapy with TAvi6 revealed that the bispecific antibody was able to suppress tumor growth in the Colo205 xenograft, which had progressed after pre-treatment with bevacizumab. This indicates that upregulation of Ang-2 may be a candidate among others for a mechanism leading to acquired resistance to bevacizumab.[32] Sustained treatment with VEGF-Trap results in constitutive VEGFR activation,[33] and TAvi6 may also be superior to other treatment options.[34,35] It was recently shown that inhibition of VEGF alone can have detrimental effects. Despite effective elimination of tumor blood vessels, tumors not only started to re-expand and the treatment may even have promoted metastasis formation.[21-23]

Compared to maintenance treatment with bevacizumab, the appearance of metastases in the lung was significantly

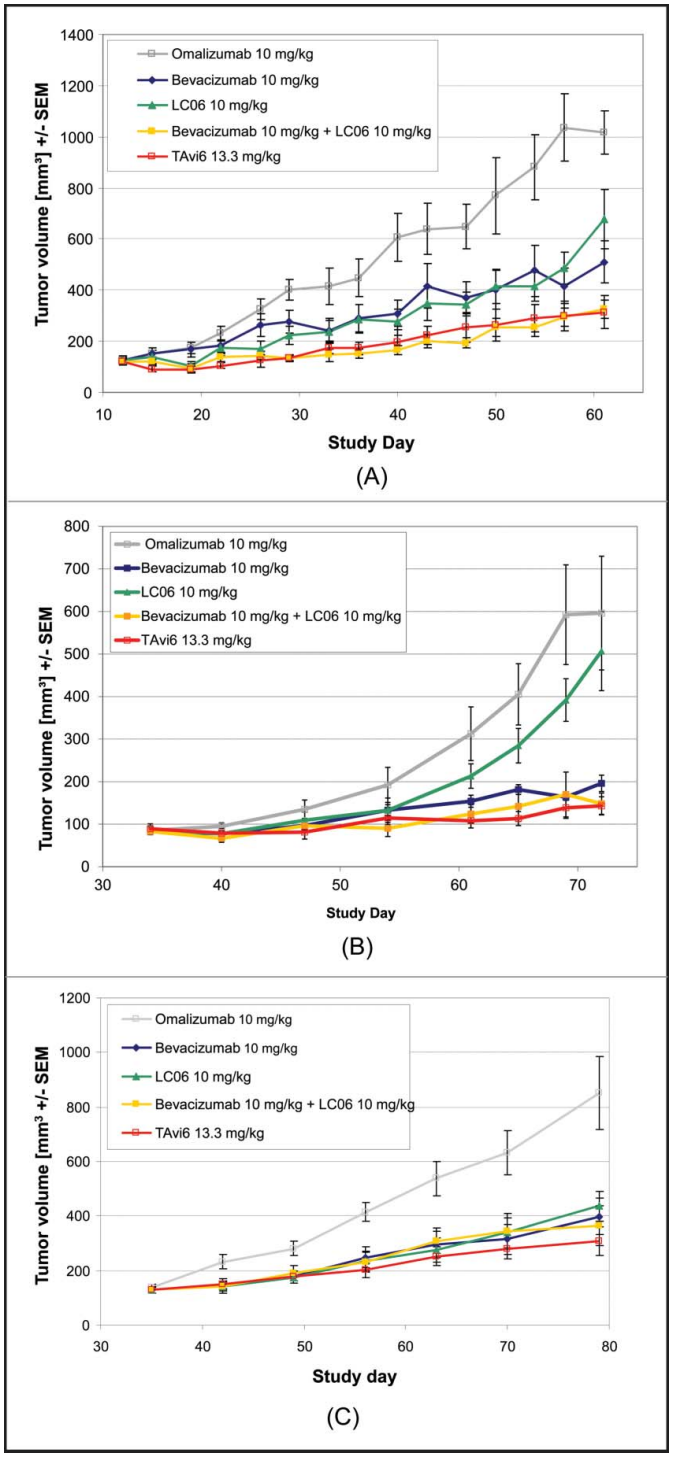

Figure 3. (A) COLO205 cells were injected s.c. into female SCID beige mice and treatment was initiated at a tumor volume of 150 mm^3. Mice (10 mice/group) were treated once weekly i.p. with the indicated doses. Omalizumab, a humanized anti-IgE antibody was used as a control. For calculation of the percentage tumor growth inhibition (TGI), every treated group was compared with its respective vehicle control. (B) KPL-4 cells were implanted orthotopically into the right penultimate inguinal mammary fat pad of female SCID beige mice. Treatment was initiated at a tumor volume of 80 mm^3 and mice ($n = 10$) were treated once weekly i.p. with the indicated doses. (C) Calu-3 cells (5×106 in 100 μl) were injected s.c. into female BALB/c nude mice. Treatment was initiated at a tumor volume of 150 mm^3. Mice were treated once weekly i.p. with the different compounds and doses as indicated. TGI for TAvi6 was 70% ($p < 0.001$).

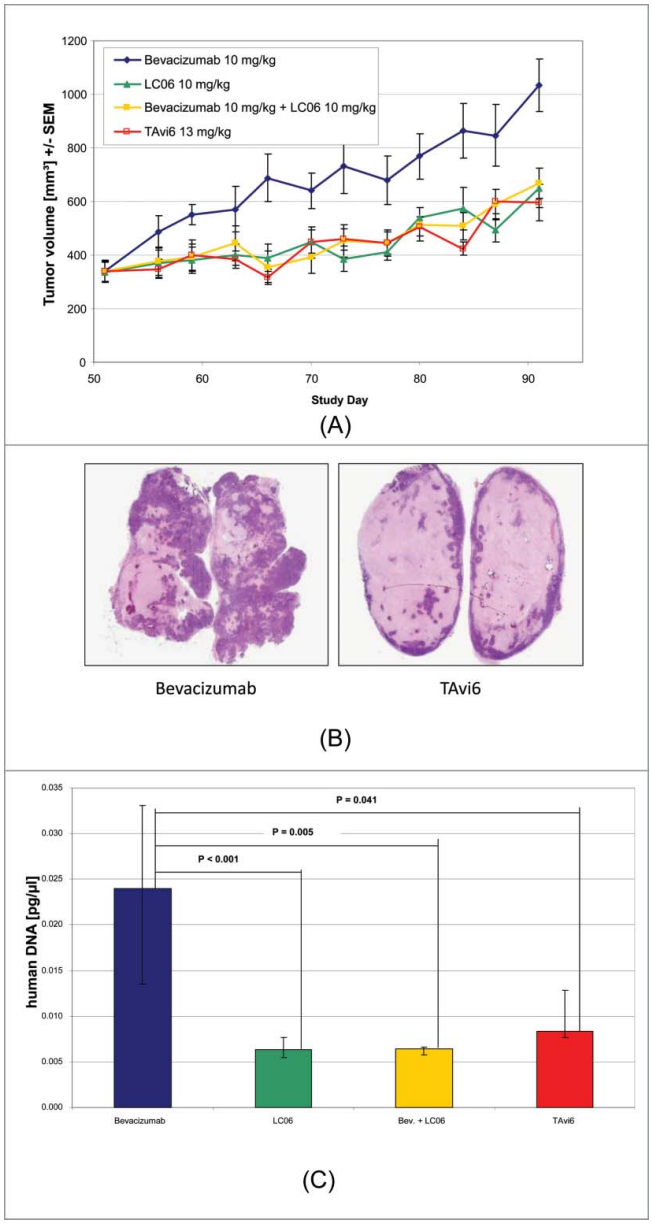

Figure 4. (A) Established Colo205 xenografts were treated with bevacizumab (once weekly 10 mg/kg i.p.) for 5 weeks. Thereafter mice were randomized based on tumor volume and subsequently treated i.p. with the compounds once weekly (10 mice/group). Compared to bevacizumab, treatment with LC06 suppressed tumor volume by 44% ($p = 0.006$), combination of bevacizumab with LC06 by 45% ($p = 0.005$) and for TAvi6 TGI was 60% ($p = 0.002$). Histology of explanted tumors revealed massive destruction of tumor cells after TAvi6 treatment. (B) Histology of explanted Colo205 tumors revealed massive cell death after TAvi6 treatment indicating superior activity of the bispecific antibody compared to bevacizumab. (C) TAvi6 suppresses metastasis to the lung in the s.c. Colo205 CRC xenograft after first-line bevacizumab. At study termination (day 91) lungs were collected from animals of all groups. Samples were transferred immediately into liquid nitrogen. DNA was isolated with a MagNA Pure LC Instrument according to manufacturer's instructions. Human Alu specific primers were chosen for selective amplification of Alu sequences by quantitative PCR. Compared to bevacizumab all compounds suppressed metastasis to the lung significantly, for TAvi6 suppression was 66%.

suppressed by second-line treatment with LC06, by treatment with the combination of bevacizumab with LC06, and with TAvi6. These results demonstrating that TAvi6 significantly suppressed primary tumor growth and the formation of metastases are in line with recent findings on the role of Ang-2 in the

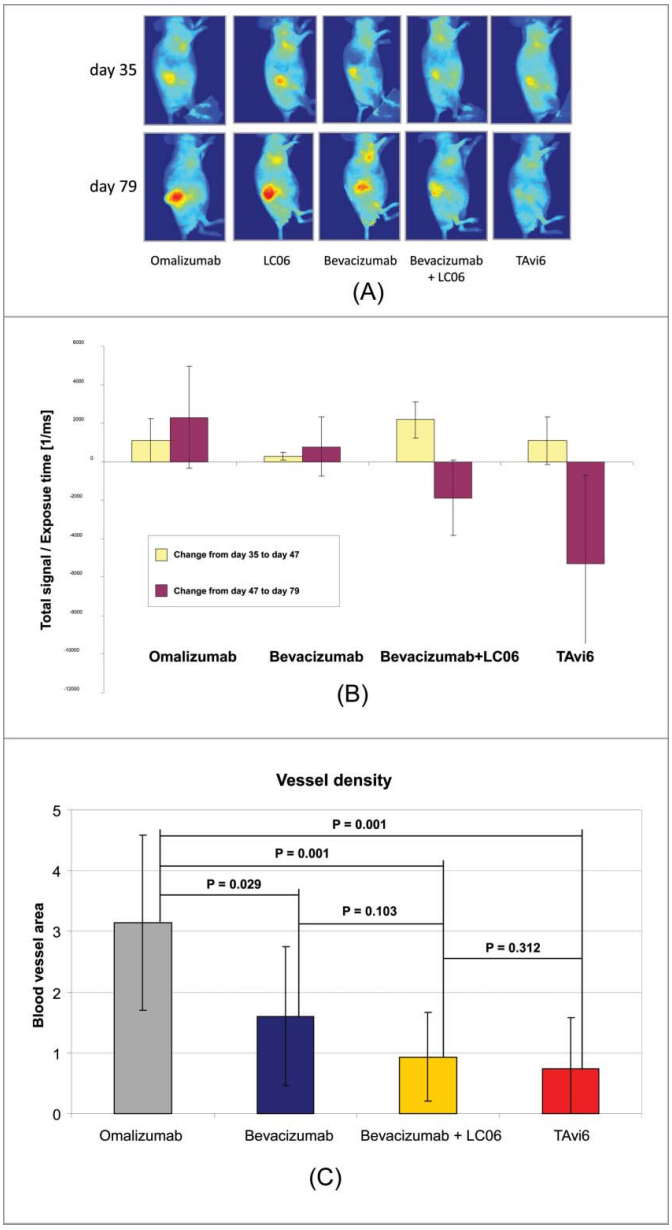

Figure 5. (A) Mice were injected with 2 mg/kg fluorescence labeled anti-CD31 i.v. on days 34 and 78. Fluorescence signal intensities were measured by planar reflectance imaging 24 hours thereafter (MAESTRO; PerkinElmer). In the omalizumab control treatment group the signal intensity became more prominent over time indicating more CD31 positive vessels in the tumor tissue. In contrast, treatment with combo (bevacizumab plus LC06) or TAvi6 reduced fluorescence intensities in the region of interest. (B) Relative change of CD31 staining. Treatment groups exhibited no significant changes of labeled anti-CD31 signals in the first 2 weeks of treatment (yellow bars: day 35 to day 47). In contrast, fluorescence signal intensities declined in mice treated with the combination and TAvi6 treated mice indicating that vessel formation is affected by these treatments (red bars: day 47 to day 79). (C) Microvessel density was quantified manually in 3 tumors from each group and 4 slides from each tumor were analyzed. Compared to omalizumab as a control all treatments suppressed vessel densities significantly and TAvi6 exerted the most prominent effect (75% inhibition).

metastasis process,[36-38] and may be of importance for the clinical situation.

Histology of explanted tumors revealed strong tumor cell death after TAvi6 treatment, and only a rim of proliferating tumor cells was left, indicating superior activity of the bispecific antibody compared to bevacizumab as single treatment. In correlation with the anti-angiogenic property of TAvi6 in the mouse cornea pocket model, angiogenesis was also inhibited in vivo. Fluorescence-labeled anti-murine CD31 was applied to monitor angiogenesis at different time points during therapy. Planar reflectance optical imaging measurements revealed prominent suppression of the fluorescence signal intensities in the tumor area compared to omalizumab as a control and treatment with LC06 and bevacizumab. Ex vivo analysis of the explanted tumor tissue by classical histology and multispectral fluorescence imaging of tissue slides confirmed these findings. There was an almost complete shut-down of vessels in the TAvi6-treated mice and microvessel density was significantly suppressed.

In summary, we describe a novel bispecific antibody targeting both Ang2 and VEGF with IgG-like properties that potently inhibited angiogenesis, suppressed tumor growth in different xenograft models comparable to the combination of the respective parental antibodies, was effective after second-line therapy with bevacizumab, and which effectively suppressed formation of metastases. Given its favorable biophysical properties and activity in preclinical models, TAvi6 has the potential to be developed as a therapeutic agent, but it ultimately was not selected for further development due to the overall superior properties and activity of vanucizumab (data not shown).

Material and methods

Antibody generation

TAvi6 (= 2441-TvAb-Avastin-LC06) is a tetravalent bispecific, humanized IgG1 antibody targeting VEGF-A and angiopoietin 2. The molecule composition is based upon the tetravalent 'Morrison format' with single-chain Fv modules added to the C-termini of the heavy chains of full-length IgGs using a (G4S) 4 connector.[24] The IgG1 part is identical to bevacizumab. Targeting Ang-2 was realized by fusing the disulfide-stabilized (VH-44 to VL-100) variable domains of the LC06 antibody[17] as scFvs using a (G4S)4 linker to the C-terminus of bevacizumab. The bispecific antibody contains stabilizing interchains in these scFv modules (VH44-VL100)[25,26] to stabilize the scFv modules and prevent aggregation.[27-29] Two molecules were generated for comparative purposes: 1) bispecific tetravalent antibody based on the human/murine VEGF cross-reactive antibody B20-4.1 termed muTAvi6,[30] and 2) bispecific monovalent Ang-2-VEGF CrossMAb with CH1-CL crossover based on LC06 and bevacizumab termed Ang-2-VEGF-CM.[31]

Cloning and expression of TAvi6

Transient transfections in HEK293-F system

Antibodies were generated by transient transfection of the 2 plasmids encoding the heavy or modified heavy chain, respectively, and the corresponding light chain using the HEK293-F system (Invitrogen) according to the manufacturer's instruction. According to the glucose consumption, glucose solution was added during the course of the fermentation. The supernatant containing the secreted antibody was harvested after 5–10 days and antibodies were purified from the supernatant.

Protein purification

Proteins were purified from filtered cell culture supernatants referring to standard protocols. In brief, antibodies were applied to a Protein A Sepharose column (GE Healthcare) and washed with PBS. Elution of antibodies was achieved at acidic pH followed by immediate neutralization of the sample. Aggregated protein was separated from monomeric antibodies by size-exclusion chromatography (Superdex 200, GE Healthcare) in 20 mM histidine, 140 mM NaCl pH 6.0. Monomeric antibody fractions were pooled, concentrated, and stored at −80°C. Part of the samples were provided for subsequent protein analytics and analytical characterization, e.g., by SDS-PAGE, size-exclusion chromatography, mass spectrometry and endotoxin determination.

SDS-PAGE

The NuPAGE® Pre-Cast gel system (Invitrogen) was used according to the manufacturer's instruction. In particular, 4-20% NuPAGE® Novex® TRIS-Glycine Pre-Cast gels and a Novex® TRIS-Glycine SDS running buffer were used under reducing conditions.

Analytical size-exclusion chromatography

Size-exclusion chromatography for the assessment of the aggregation and oligomeric state was performed by high performance liquid chromatography (HPLC) using a Tosoh TSKgel G3000SW column in 300 mM NaCl, 50 mM KH_2PO_4/K_2HPO_4, pH 7.5 or a Superdex 200 column (GE Healthcare) in 2 × PBS. The eluted protein was quantified by UV absorbance and integration of peak areas.

Dynamic light scattering

Samples were prepared at 1 mg/mL in 20 mM histidine chloride, 140 mM NaCl, pH 6.0. Samples were filtered through a 0.4 μm filter, overlaid with paraffin oil and heated in a DynaPro plate reader (Wyatt Inc., Santa Barbara/USA) from 25 to 80°C at a rate of 0.02°C/minute. The aggregation onset temperature (Tagg) was defined as the temperature at which the average hydrodynamic radius begins to increase.

Generation and selection of TAvi6 expressing CHO cell lines

CHO K1-SV cells were transfected by electroporation (Biorad) with linearized plasmid DNA expressing both bispecific antibody chains. Cell were cultivated for 48 h in CD-CHO medium (Invitrogen) supplemented with GS Supplement (Gibco), L-glutathione (Sigma Aldrich), and Ac-Cys-OH (Bachem) Two days after transfection cells were seeded into 384-well plates and cultivated for 2 weeks in CD-CHO medium supplemented with 75 μM MSX to select stably transfected cells. Wells containing stably transfected cells were identified by a high-throughput ELISA screening detecting the Fc part of the bispecific antibody. Parental clones expressing high levels of bispecific antibody were expanded into shake flasks and further analyzed in batch and fed-batch cultivation mode. Parental clone TAvi6_477 was selected for production of bispecific antibody in 20 L and 100 L fermenters.

Ang-2 and VEGF binding kinetics

Binding kinetics was analyzed by SPR technology using a Biacore T100 instrument (GE Healthcare). Goat anti-human Fc IgG (Jackson ImmunoResearch) was immobilized on the surface of a CM4 (for Ang-2 binding) or a C1 (for VEGF binding) sensor chip using standard amine-coupling chemistry resulting a surface density of ~ 500 RU (CM4) and 200 RU (C1). A reference flow cell was treated in the same way. The antibodies were diluted in running buffer (10 mM HEPES, 150 mM NaCl, 0.05% PS 20 containing 1 mg/ml bovine serum albumin) and injected at a flow rate of 5 μl/min. The contact time (association phase) was 1 min for the antibodies at a concentration of 10 nM. Ang-2 or VEGF were injected at increasing concentrations. The contact time (association phase) was 3 min, the dissociation time (washing with running buffer) 5 min for both molecules at a flowrate of 30 μl/min. All interactions were performed at 25°C (standard temperature). The regeneration solutions of 0.85% phosphoric acid, followed by 5 mM sodium hydroxide were injected for 60 s at 5 μl/min flow rate to remove any non-covalently bound protein after each binding cycle. The derived curves were fitted to a 1:1 Langmuir binding model using the BIAevaluation software (GE Healthcare).

Simultaneous, independent binding was confirmed by SPR. A goat anti-human Fc antibody (Jackson ImmunoResearch) was immobilized on a C1 Sensorchip using standard amine coupling chemistry. In a first step, the bivalent antibody was injected at a concentration of 5 nM in HBS buffer. After binding of the antibody, either hAng-2 or VEGF was injected followed by a second injection of VEGF or hAng-2. Additionally, each antigen was injected alone. HBS buffer (10 mM HEPES, 150 mM NaCl, 0.05% Tween 20, pH 7.4) was used as running and dilution buffer at a temperature of 25°C.

Phospho-Tie2 assay

HEK293 (German Collection of Microorganisms and Cell Lines, DSMZ, Braunschweig) suspension cells overexpressing the angiopoietin-2 receptorTie-2 were added as 2 × 10^5 cells/well to the pre-incubated mixture of dilution series of the bispecific antibody and 120 ng/well Ang-2 (R&D Systems). After 10 minutes at room temperature (RT), the cells were lysed and incubated at 2 – 8°C for 15 min. The cell lysate was transferred to an ELISA plate. The ELISA plates (Maxisorb, Nunc) were pre-coated with antibody against human Tie-2 receptor (R&D Systems) used as a capture antibody. The phosphorylated tyrosines were detected by anti-phosphotyrosine antibody conjugated to biotin (Upstate) through a streptavidin-HRP conjugate (Roche Applied Science). The peroxidase substrate TMB (Roche Applied Science) was added and the optical density was measured at 450 nm. The O.D. values correlated with the amount of phosphorylated Tie-2 and were plotted against the TAvi6 concentrations. The XLfit program was used to fit a 4-parameter curve.

Ang2-Tie2 interaction ELISA

The ELISA test for inhibition of huAngiopoietin-2/1 binding to Tie-2 was performed on 384-well microtiter plates (MicroCoat) at RT. After each incubation step plates were washed 3 times with PBST. At the beginning, plates were coated with 0.5 μg/ml Tie-2 protein (R&D Systems) for at least 2 h. Thereafter the wells were blocked with PBS supplemented with 0.2% Tween-20 and 2% BSA for 1 h. Dilutions of purified antibodies in PBS were incubated together with 0.2 μg/ml huAng-2 (R&D Systems) or with 0.2 μg/ml huAng-1 (R&D Systems) for 1 h at RT. After washing a mixture of 0.5 μg/ml biotinylated anti-Angiopoietin clone BAM0981 (R&D Systems) and 1:3000 diluted streptavidin HRP (Roche Diagnostics) was added for 1 h. Thereafter the plates were washed 6 times with PBST. Plates were developed with freshly prepared ABTS reagent for 30 minutes at RT. Absorbance was measured at 405 nm.

Ang2-Tie2 inhibition FACS

Tavi6 antibodies at different concentrations were pre-incubated with recombinant human Ang-2 (R&D Systems) at 1.25 μg/mL for 15 min (RT) before adding the mixture to 3×10^5 HEK293-Tie2 cells in a total volume of 120 μl. After 2 h incubation on ice, cells were washed twice with cold PBS/2% fetal calf serum (FCS) and then incubated for another 45 min with biotinylated anti-human Ang2 (R&D Systems) at 5 μg/mL, followed by 2 washes and a third incubation with PE-coupled streptavidin (Life Technologies) for 45 min on ice. Subsequently, cells were washed twice, re-suspended in FACS buffer and Ang-2 binding quantified on a FACS-Canto flow cytometer (Becton Dickinson).

VEGF induced HUVEC proliferation assay

VEGF-induced human umbilical vein endothelial cells (HUVEC; Promocell) proliferation was chosen to measure the cellular activity of the different antibodies. Briefly, 5000 HUVEC cells (low passage number, $\leq$5 passages) per well of a 96-well plate were incubated in 100 μl starvation medium (EBM-2 endothelial basal medium 2, Promocell) in a collagen I-coated BD Biocoat CollagenI 96-well microtiter plate (BD) overnight. Varying concentrations of antibody were mixed with hVEGF (30 ng/ml, BD) and pre-incubated for 15 minutes at RT. Subsequently, the mix was added to the HUVEC cells and they were incubated for 72 h. On the day of analysis the plate was equilibrated to RT for 30 min and cell viability/proliferation was determined using the CellTiter-Glo Luminescent Cell Viability Assay kit according to the manual (Promega). Luminescence was determined in a spectrophotometer.

Inhibition of huVEGF binding to huVEGF receptor

The ELISA test was performed on 384-well microtiter plates (MicroCoat) at RT. After each incubation step, plates were washed 3 times with PBST. At the beginning, plates were coated with 0.5 μg/ml huVEGF-R protein (R&D Systems) for at least 2 h. Thereafter the wells were blocked with PBS supplemented with 0.2% Tween-20 and 2% BSA for 1 h. Dilutions of purified antibodies in PBS were incubated together with 0.15 μg/ml huVEGF121 (R&D Systems) for 1 h at RT. After washing a mixture of 0.5 μg/ml anti-VEGF clone Mab923 (R&D Systems) and 1:2000 HRP-conjugated F(ab′)2 anti-mouse IgG (GE Healthcare) was added for 1 h. Thereafter the plates were washed 6 times with PBST. Plates were developed with freshly prepared ABTS reagent for 30 minutes at RT. Absorbance was measured at 405 nm.

Corneal micropocket model

The protocol was modified according to the method described by Rogers et al.[39] Briefly, micropockets were prepared under a microscope at ~1 mm from the limbus to the top of the cornea using a surgical blade and sharp tweezers in the anesthetized mouse. The disc (Nylaflo®, Pall Corporation) was implanted and the surface of the implantation area was smoothened. Discs were incubated in VEGF-A or in vehicle for at least 30 min. After 5 days, eyes were photographed and vascular response was measured. The assay was quantified by expressing the area of new vessels as a fraction of the total area of the cornea. LC06, bevacizumab and TAvi6 were injected with 10 mg/kg i.v. at the day of disc implantation. The experimental study protocol was reviewed and approved by the Bavarian government (approval number AZ 55.2-1-54-2531.2-34-08).

Cell lines and cell culture

Colo205 human colorectal cancer cells were obtained from ATCC and cultured in RPMI 1640 containing 10% FCS, 2 mM Lglutamine. The human breast cancer cell line KPL-4 (Prof. J. Kurebayashi, Kawasaki Medical School, Kurashiki, Japan) was routinely cultured in DMEM supplemented with 10% FCS and 2 mM L-glutamine.[40] The NSCLC tumor cells Calu-3 were obtained from Chugai Pharmaceuticals Co., Ltd. and cultured. Cell viability was assessed using a cell counter and analyzer system (Vi-CELL, Beckman Coulter) and viability was ca. 95%.

Tumor xenografts

To initiate tumor xenografts, Colo205 cells (2.5 × 10e6 cells/100 μl PBS) were injected s.c. into the right flank of female SCID beige mice (Charles River Germany). KPL-4 cells (3 × 10e6/20 μl PBS) were implanted orthotopically into the right penultimate inguinal mammary fat pad of female SCID beige mice. Calu-3 cells (5 × 10e6/PBS) were injected s.c. into BALB/c nu/nu female mice (Charles River Germany). Tumor cells were injected into anesthetized mice and tumors were allowed to establish growth after implantation before initiation of treatment. Body weight of mice and tumor volume were monitored twice weekly and the formula to calculate tumor volume used is an approximation for the calculation of elliptical shaped tumors. It comprises the length L (longest dimension) and width W (shorter dimension) of the tumors [$(V = 0.5\times L\times (W^2)$]. All experimental study protocols were reviewed and approved by local government (AZ 55.2-1-54-2531.2-26-09 and AZ 55.2-1-54-2531.2-3-08). Mice were handled according

to committee guidelines (GV-Solas; Felasa; TierschG) and the animal facility has been accredited by AALAAC.

Treatment of animals

Treatment started at day of randomization. Mice were treated once weekly i.p. with equimolar doses as indicated in the Figure legends. Omalizumab, a humanized IgG1 antibody targeting human IgE served as a specificity control. After sacrificing the animals, tumors were explanted and transferred into an embedding cassette for histological analysis or flash frozen in liquid nitrogen for PCR applications.

Near-infrared optical imaging

An anti-mouse CD31 monoclonal antibody (ACRIS Antibodies) was labeled with the fluorescent dye Alexa610 (Invitrogen) according to the manufacturer's instructions. After the coupling procedure, antibody was purified from free dye by HPLC (purity >95%) and the labeling ratio was quantified (Alexa/antibody 1.7:1). Mice were injected i.v. with a single 50-μg dose of the fluorescence labeled antibody at day 34 and day 78. Near infrared planar reflectance imaging measurements were performed 24 hrs thereafter using the MAESTRO Imaging System (PerkinElmer) equipped with an inhalation mask for anesthesia. Fluorescence signal intensities in the region of interest were quantified by the MAESTRO software according to the manufacturer's instructions.

Histology und fluorescence microscopy

Explanted tumors were enclosed in an embedding cassette and were incubated under continuous agitation in formalin for $\sim$ 24 hours. Thereafter, formalin was discarded and tumors washed with distilled water followed by dehydration of the tumors and penetration of paraffin according to established methods. All the incubation steps were carried out using the Tissue Tek® VIP Vacuum Infiltration Processor. After paraffin penetration, tumors were embedded in liquid paraffin with the Tissue Tek® Paraffin embedding station to a final histological block. Paraffin sections in a range of 2 – 8 μm of thickness were obtained from these blocks using a microtome. Slides were examined by classical microscopy (HE) and multispectral fluorescence microscopy with the NUANCE system (CRi). Based on fluorescence microscopy vessels were quantified manually in 3 tumors from each group and 4 slides from each tumor were analyzed.

Assessment of disseminated tumor cells by quantification of human DNA (Alu-PCR)

After termination of the experiments mice were sacrificed by cervical dislocation, lungs were excised and put immediately in liquid nitrogen. Quantitative assessment of disseminated tumor cells was achieved by using human-specific Alu repeats detecting human tumor DNA. Genomic DNA from the lungs of mice was isolated using the High Pure PCR Template Preparation kit (Roche Diagnostics GmbH) and quantified using the PicoGreen Quantification kit (Molecular Probes) according to the manufacturer's instructions. Primers for human Alu repeats were synthesized by TIB MOLBIOL GmbH and quantitative PCR (qPCR) was performed using the Light-Cycler System (Roche Diagnostics GmbH), as previously described.[41] Results are displayed as pg human DNA per 2.5 ng total DNA.

Statistical analysis

Results of corneal angiogenesis assay and xenograft experiments were expressed as mean±SEM. Differences between experimental groups were analyzed by unpaired Student's t-test and p values < 0.05 were considered statistically significant. Tumor growth inhibition was assessed by the formula:

$$TGI\,[\%] = 100 - \frac{median(TV(treated)_{day\,z} - TV(treated)_{day\,x})}{median(TV(resp.\,control)_{day\,z} - TV(resp.\,control)_{day\,x})} \times 100.$$

In a randomized 2-sample design, the parametric tumor-control ratio (TCR) and its 2-sided non-parametric 95% confidence interval were calculated using the following formula along with Fieller's CI for ratios.[42]

$$TCR = \frac{\overline{V}_{treated}}{\overline{V}_{control}}.$$

Disclosure of potential conflicts of interest

All authors are employees of Roche.

Acknowledgment

We would like to thank Ute Haupt and Rosa-Maria Busl for their valuable technical expertise.

References

1. Bergers G, Hanahan D. Modes of resistance to anti-angiogenic therapy. Nat Rev Cancer 2008; 8(8):592-603; PMID:18650835; http://dx.doi.org/10.1038/nrc2442
2. Crawford Y, Ferrara N. Vegf inhibition: Insights from preclinical and clinical studies. Cell Tissue Res 2009; 335(1):261-9; PMID:18766380; http://dx.doi.org/10.1007/s00441-008-0675-8
3. Hodi FS, Lawrence D, Lezcano C, Wu X, Zhou J, Sasada T, Zeng W, Giobbie-Hurder A, Atkins MB, Ibrahim N, et al. Bevacizumab plus ipilimumab in patients with metastatic melanoma. Cancer Immunol Res 2014; 2(7):632-42; PMID:24838938; http://dx.doi.org/10.1158/2326-6066.CIR-14-0053
4. Ma J, Waxman DJ. Combination of antiangiogenesis with chemotherapy for more effective cancer treatment. Mol Cancer Ther 2008; 7(12):3670-84; PMID:19074844; http://dx.doi.org/10.1158/1535-7163.MCT-08-0715
5. Jubb AM, Harris AL. Biomarkers to predict the clinical efficacy of bevacizumab in cancer. Lancet Oncol 2010; 11(12):1172-83; PMID:21126687; http://dx.doi.org/10.1016/S1470-2045(10)70232-1
6. Fernando NT, Koch M, Rothrock C, Gollogly LK, D'Amore PA, Ryeom S, Yoon SS. Tumor escape from endogenous, extracellular matrix-associated angiogenesis inhibitors by up-regulation of multiple proangiogenic factors. Clin Cancer Res 2008; 14(5):1529-39; PMID:18316578; http://dx.doi.org/10.1158/1078-0432.CCR-07-4126

7. Daly C, Eichten A, Castanaro C, Pasnikowski E, Adler A, Lalani AS, Papadopoulos N, Kyle AH, Minchinton AI, Yancopoulos GD, et al. Angiopoietin-2 functions as a tie2 agonist in tumor models, where it limits the effects of vegf inhibition. Cancer Res 2013; 73 (1):108-18; PMID:23149917; http://dx.doi.org/10.1158/0008-5472.CAN-12-2064
8. Kienast Y, Klein C, Scheuer W, Raemsch R, Lorenzon E, Bernicke D, Herting F, Yu S, The HH, Martarello L, et al. Ang-2-vegf-a crossmab, a novel bispecific human igg1 antibody blocking vegf-a and ang-2 functions simultaneously, mediates potent antitumor, antiangiogenic, and antimetastatic efficacy. Clin Cancer Res 2013; 19(24):6730-40; PMID:24097868; http://dx.doi.org/10.1158/1078-0432.CCR-13-0081
9. Scholz A, Harter PN, Cremer S, Yalcin BH, Gurnik S, Yamaji M, Di Tacchio M, Sommer K, Baumgarten P, Bahr O, et al. Endothelial cell-derived angiopoietin-2 is a therapeutic target in treatment-naive and bevacizumab-resistant glioblastoma. EMBO Mol Med 2015; 8(1):39-57; PMID:26666269; http://dx.doi.org/10.15252/emmm.201505505
10. Xu L, Duda DG, di Tomaso E, Ancukiewicz M, Chung DC, Lauwers GY, Samuel R, Shellito P, Czito BG, Lin PC, et al. Direct evidence that bevacizumab, an anti-vegf antibody, up-regulates sdf1alpha, cxcr4, cxcl6, and neuropilin 1 in tumors from patients with rectal cancer. Cancer Res 2009; 69(20):7905-10; PMID:19826039; http://dx.doi.org/10.1158/0008-5472.CAN-09-2099
11. Brown JL, Cao ZA, Pinzon-Ortiz M, Kendrew J, Reimer C, Wen S, Zhou JQ, Tabrizi M, Emery S, McDermott B, et al. A human monoclonal anti-ang2 antibody leads to broad antitumor activity in combination with vegf inhibitors and chemotherapy agents in preclinical models. Mol Cancer Ther 2010; 9(1):145-56; PMID:20053776; http://dx.doi.org/10.1158/1535-7163.MCT-09-0554
12. Huang H, Lai JY, Do J, Liu D, Li L, Del Rosario J, Doppalapudi VR, Pirie-Shepherd S, Levin N, Bradshaw C, et al. Specifically targeting angiopoietin-2 inhibits angiogenesis, tie2-expressing monocyte infiltration, and tumor growth. Clin Cancer Res 2011; 17(5):1001-11; PMID:21233403; http://dx.doi.org/10.1158/1078-0432.CCR-10-2317
13. Leow CC, Coffman K, Inigo I, Breen S, Czapiga M, Soukharev S, Gingles N, Peterson N, Fazenbaker C, Woods R, et al. Medi3617, a human anti-angiopoietin 2 monoclonal antibody, inhibits angiogenesis and tumor growth in human tumor xenograft models. Int J Oncol 2012; 40(5):1321-30; PMID:22327175; http://dx.doi.org/10.3892/ijo.2012.1366
14. Papadopoulos KP, Kelley RK, Tolcher AW, Razak AR, Van Loon K, Patnaik A, Bedard PL, Alfaro AA, Beeram M, Adriaens L, et al. A phase i first-in-human study of nesvacumab (regn910), a fully human anti-angiopoietin-2 (ang2) monoclonal antibody, in patients with advanced solid tumors. Clin Cancer Res 2015; PMID:26490310
15. Mazzieri R, Pucci F, Moi D, Zonari E, Ranghetti A, Berti A, Politi LS, Gentner B, Brown JL, Naldini L, et al. Targeting the ang2/tie2 axis inhibits tumor growth and metastasis by impairing angiogenesis and disabling rebounds of proangiogenic myeloid cells. Cancer Cell 2011; 19(4):512-26; PMID:21481792; http://dx.doi.org/10.1016/j.ccr.2011.02.005
16. Oliner J, Min H, Leal J, Yu D, Rao S, You E, Tang X, Kim H, Meyer S, Han SJ, et al. Suppression of angiogenesis and tumor growth by selective inhibition of angiopoietin-2. Cancer Cell 2004; 6(5):507-16; PMID:15542434; http://dx.doi.org/10.1016/j.ccr.2004.09.030
17. Thomas M, Kienast Y, Scheuer W, Bahner M, Kaluza K, Gassner C, Herting F, Brinkmann U, Seeber S, Kavlie A, et al. A novel angiopoietin-2 selective fully human antibody with potent anti-tumoral and anti-angiogenic efficacy and superior side effect profile compared to pan-angiopoietin-1/-2 inhibitors. PLoS One 2013; 8(2):e54923; PMID:23405099; http://dx.doi.org/10.1371/journal.pone.0054923
18. Gerald D, Chintharlapalli S, Augustin HG, Benjamin LE. Angiopoietin-2: An attractive target for improved antiangiogenic tumor therapy. Cancer Res 2013; 73(6):1649-57; PMID:23467610; http://dx.doi.org/10.1158/0008-5472.CAN-12-4697
19. Hashizume H, Falcon BL, Kuroda T, Baluk P, Coxon A, Yu D, Bready JV, Oliner JD, McDonald DM. Complementary actions of inhibitors of angiopoietin-2 and vegf on tumor angiogenesis and growth. Cancer Res 2010; 70(6):2213-23; PMID:20197469; http://dx.doi.org/10.1158/0008-5472.CAN-09-1977
20. Doppalapudi VR, Huang J, Liu D, Jin P, Liu B, Li L, Desharnais J, Hagen C, Levin NJ, Shields MJ, et al. Chemical generation of bispecific antibodies. Proc Natl Acad Sci U S A 2010; 107(52):22611-16; PMID:21149738; http://dx.doi.org/10.1073/pnas.1016478108
21. Ebos JM, Lee CR, Cruz-Munoz W, Bjarnason GA, Christensen JG, Kerbel RS. Accelerated metastasis after short-term treatment with a potent inhibitor of tumor angiogenesis. Cancer Cell 2009; 15(3):232-9; PMID:19249681; http://dx.doi.org/10.1016/j.ccr.2009.01.021
22. Loges S, Mazzone M, Hohensinner P, Carmeliet P. Silencing or fueling metastasis with vegf inhibitors: Antiangiogenesis revisited. Cancer Cell 2009; 15(3):167-70; PMID:19249675; http://dx.doi.org/10.1016/j.ccr.2009.02.007
23. Paez-Ribes M, Allen E, Hudock J, Takeda T, Okuyama H, Vinals F, Inoue M, Bergers G, Hanahan D, Casanovas O. Antiangiogenic therapy elicits malignant progression of tumors to increased local invasion and distant metastasis. Cancer Cell 2009; 15(3):220-31; PMID:19249680; http://dx.doi.org/10.1016/j.ccr.2009.01.027
24. Coloma MJ, Morrison SL. Design and production of novel tetravalent bispecific antibodies. Nat Biotechnol 1997; 15(2):159-63; PMID:9035142; http://dx.doi.org/10.1038/nbt0297-159
25. Reiter Y, Brinkmann U, Kreitman RJ, Jung SH, Lee B, Pastan I. Stabilization of the fv fragments in recombinant immunotoxins by disulfide bonds engineered into conserved framework regions. Biochemistry 1994; 33(18):5451-59; PMID:7910034; http://dx.doi.org/10.1021/bi00184a014
26. Reiter Y, Brinkmann U, Webber KO, Jung SH, Lee B, Pastan I. Engineering interchain disulfide bonds into conserved framework regions of fv fragments: Improved biochemical characteristics of recombinant immunotoxins containing disulfide-stabilized fv. Protein Eng 1994; 7(5):697-704; PMID:8073039; http://dx.doi.org/10.1093/protein/7.5.697
27. Metz S, Haas AK, Daub K, Croasdale R, Stracke J, Lau W, Georges G, Josel HP, Dziadek S, Hopfner KP, et al. Bispecific digoxigenin-binding antibodies for targeted payload delivery. Proc Natl Acad Sci U S A 2011; 108(20):8194-99; PMID:21536919; http://dx.doi.org/10.1073/pnas.1018565108
28. Croasdale R, Wartha K, Schanzer JM, Kuenkele KP, Ries C, Mayer K, Gassner C, Wagner M, Dimoudis N, Herter S, et al. Development of tetravalent igg1 dual targeting igf-1r-egfr antibodies with potent tumor inhibition. Arch Biochem Biophys 2012; 526(2):206-18; PMID:22464987; http://dx.doi.org/10.1016/j.abb.2012.03.016
29. Schanzer J, Jekle A, Nezu J, Lochner A, Croasdale R, Dioszegi M, Zhang J, Hoffmann E, Dormeyer W, Stracke J, et al. Development of tetravalent, bispecific ccr5 antibodies with antiviral activity against ccr5 monoclonal antibody-resistant hiv-1 strains. Antimicrob Agents Chemother 2011; 55(5):2369-78; PMID:21300827; http://dx.doi.org/10.1128/AAC.00215-10
30. Liang WC, Wu X, Peale FV, Lee CV, Meng YG, Gutierrez J, Fu L, Malik AK, Gerber HP, Ferrara N, et al. Cross-species vascular endothelial growth factor (vegf)-blocking antibodies completely inhibit the growth of human tumor xenografts and measure the contribution of stromal vegf. J Biol Chem 2006; 281(2):951-61; PMID:16278208; http://dx.doi.org/10.1074/jbc.M508199200
31. Schaefer W, Regula JT, Bahner M, Schanzer J, Croasdale R, Durr H, Gassner C, Georges G, Kettenberger H, Imhof-Jung S, et al. Immunoglobulin domain crossover as a generic approach for the production of bispecific igg antibodies. Proc Natl Acad Sci U S A 2011; 108 (27):11187-92; PMID:21690412; http://dx.doi.org/10.1073/pnas.1019002108
32. Rigamonti N, Kadioglu E, Keklikoglou I, Wyser Rmili C, Leow CC, De Palma M. Role of angiopoietin-2 in adaptive tumor resistance to vegf signaling blockade. Cell Rep 2014; 8(3):696-706; PMID:25088418; http://dx.doi.org/10.1016/j.celrep.2014.06.059
33. Kadenhe-Chiweshe A, Papa J, McCrudden KW, Frischer J, Bae JO, Huang J, Fisher J, Lefkowitch JH, Feirt N, Rudge J, et al. Sustained vegf blockade results in microenvironmental sequestration of vegf by tumors and persistent vegf receptor-2 activation. Mol Cancer Res 2008; 6(1):1-9; PMID:18234958; http://dx.doi.org/10.1158/1541-7786.MCR-07-0101

34. Dempke WC, Zippel R. Brivanib, a novel dual vegf-r2/bfgf-r inhibitor. Anticancer Res 2010; 30(11):4477-83; PMID:21115896
35. Zaghloul N, Hernandez SL, Bae JO, Huang J, Fisher JC, Lee A, Kadenhe-Chiweshe A, Kandel JJ, Yamashiro DJ. Vascular endothelial growth factor blockade rapidly elicits alternative proangiogenic pathways in neuroblastoma. Int J Oncol 2009; 34(2):401-7; PMID:19148474; http://dx.doi.org/10.3892/ijo_00000163
36. Rigamonti N, De Palma M. A role for angiopoietin-2 in organ-specific metastasis. Cell Rep 2013; 4(4):621-3; PMID:23993444; http://dx.doi.org/10.1016/j.celrep.2013.07.034
37. Srivastava K, Hu J, Korn C, Savant S, Teichert M, Kapel SS, Jugold M, Besemfelder E, Thomas M, Pasparakis M, et al. Postsurgical adjuvant tumor therapy by combining anti-angiopoietin-2 and metronomic chemotherapy limits metastatic growth. Cancer Cell 2014; 26(6):880-95; PMID:25490450; http://dx.doi.org/10.1016/j.ccell.2014.11.005
38. Keskin D, Kim J, Cooke VG, Wu CC, Sugimoto H, Gu C, De Palma M, Kalluri R, LeBleu VS. Targeting vascular pericytes in hypoxic tumors increases lung metastasis via angiopoietin-2. Cell Rep 2015; 10(7):1066-81; PMID:25704811; http://dx.doi.org/10.1016/j.celrep.2015.01.035
39. Rogers MS, Birsner AE, D'Amato RJ. The mouse cornea micropocket angiogenesis assay. Nat Protoc 2007; 2(10):2545-50; PMID:17947997; http://dx.doi.org/10.1038/nprot.2007.368
40. Kurebayashi J, Otsuki T, Tang CK, Kurosumi M, Yamamoto S, Tanaka K, Mochizuki M, Nakamura H, Sonoo H. Isolation and characterization of a new human breast cancer cell line, kpl-4, expressing the erb b family receptors and interleukin-6. Br J Cancer 1999; 79(5-6):707-17; PMID:10070858; http://dx.doi.org/10.1038/sj.bjc.6690114
41. Schneider T, Osl F, Friess T, Stockinger H, Scheuer WV. Quantification of human alu sequences by real-time pcr–an improved method to measure therapeutic efficacy of anti-metastatic drugs in human xenotransplants. Clin Exp Metastasis 2002; 19(7):571-82; PMID:12498386; http://dx.doi.org/10.1023/A:1020992411420
42. Fieller E. Some problems in interval estimation. J Royal Stat Soc 1954; B16; 16:2